NASA TECHNICAL MEMORANDUM

NASA TM X-1636

NASA TM X-1636

WATER CONDENSATION EFFECTS OF HEATED VITIATED AIR ON FLOW IN A LARGE SUPERSONIC WIND TUNNEL

by Robert W. Cubbison and Edward T. Meleason

Lewis Research Center
Cleveland, Ohio

NATIONAL AERONAUTICS AND SPACE ADMINISTRATION • WASHINGTON, D. C. • AUGUST 1968

NASA TM X-1636

WATER CONDENSATION EFFECTS OF HEATED VITIATED AIR ON FLOW IN A LARGE SUPERSONIC WIND TUNNEL

By Robert W. Cubbison and Edward T. Meleason

Lewis Research Center
Cleveland, Ohio

NATIONAL AERONAUTICS AND SPACE ADMINISTRATION

For sale by the Clearinghouse for Federal Scientific and Technical Information
Springfield, Virginia 22151 – CFSTI price $3.00

ABSTRACT

Natural gas was burned directly in the air stream of the Lewis 10- by 10-foot supersonic wind tunnel to control stagnation temperature. The test-section Mach number was varied from 2.0 to 3.5, and stagnation temperature was varied to a maximum of 1140° R (634 K). Condensation of water vapor in the nozzle caused a decrease in test-section Mach number and total pressure which was repeatable and accurately calibrated. The uniformity of the flow in the test section was similar to that of the unheated air.

WATER CONDENSATION EFFECTS OF HEATED VITIATED AIR ON FLOW IN A LARGE SUPERSONIC WIND TUNNEL

by Robert W. Cubbison and Edward T. Meleason

Lewis Research Center

SUMMARY

Natural gas was burned directly in the air stream of the Lewis 10- by 10-foot supersonic wind tunnel to control stagnation temperature. The test-section Mach number was varied from 2.0 to 3.5, and stagnation temperature was varied to a maximum of 1140° R (634 K). Condensation of water vapor in the nozzle caused a decrease in test-section Mach number and total pressure which was repeatable and accurately calibrated. The uniformity of the flow in the test section was similar to that of the unheated air.

INTRODUCTION

To achieve a better simulation of actual flight conditions, airflow stagnation temperature control is required in wind tunnel tests of complete airbreathing propulsion systems. In particular, temperature affects the inlet and turbojet engine airflow matching, and it affects the combustion characteristics and fuel-flow control requirements of turbojet and ramjet engines. Free-flight temperature becomes increasingly difficult to achieve at simulated flight speeds above Mach 2 because of the rapid increase in stagnation temperature. Although heat exchangers can be used for this purpose, their initial cost is high for large facilities, and operational problems exist. A vitiated air concept utilizing direct combustion in the tunnel airflow, however, has a low initial cost, and its operation is simple, reliable, and inexpensive. Potential disadvantages are the changes in chemical composition of the heated airflow and the possibility of flow nonuniformities resulting from water-vapor condensation as the flow is expanded to supersonic velocities.

The Lewis 10- by 10-foot supersonic wind tunnel utilizes a vitiated air heater wherein natural gas is burned in the tunnel airflow just prior to its expansion in the nozzle. Because only limited data are available defining the consequences of using vitiated air in a large supersonic wind tunnel, results obtained in this particular facility are presented.

SYMBOLS

M Mach number

P total pressure

T total temperature

γ ratio of specific heats

Subscripts:

B bellmouth

l local

w wall

0 free stream

1 local total pressure behind a normal shock

2 local total pressure behind the wedge oblique shock and a normal shock

Superscript:

— average

APPARATUS AND PROCEDURE

A schematic diagram of the overall design of the 10- by 10-foot supersonic wind tunnel is presented in figure 1(a). The wind tunnel can be operated on a closed cycle for aerodynamic tests or on an open cycle for propulsion tests. In the open-cycle mode, all of the tunnel airflow, including the research propulsion-system exhaust gases, is discharged to the atmosphere rather than being recirculated. In the open-cycle mode, the direct combustion heater shown in figure 1(b) can be used to control test-section total temperature. For the data presented in this report, the atmospheric air was dried to a dew point less than -20° F (244.4 K) by the tunnel dryer prior to combustion.

A diagram of the nozzle and test section is presented in figure 2. The test-section side walls diverge $0^{\circ}22'$ each for a total width of 10.51 feet (3.2 m) at the exit to compensate for boundary layer growth. Although the test section is 40 feet (12.18 m) long, the two stations corresponding to the upstream and downstream schlieren window positions are of principal interest. Details of the flow were surveyed at several stations in the test section. However, only the results obtained at the two schlieren window positions are presented in this report.

Variations of tunnel airflow total temperature with free-stream Mach number are shown in figure 3. The minimum tunnel temperature variation is that resulting without heater operation. The jump in temperature at Mach 2.5 is the result of initiating opera-

tion of the secondary compressor. The main compressor is in operation at all speeds. The flight stagnation temperature variation in the tropopause is also shown in figure 3 for reference . The difference between these curves is equal to the temperature rise required of the heater to simulate flight. The heater was designed to equal or exceed this required temperature rise up to the design limit of 1140° R (634 K). Although even higher temperatures can be provided, it is limited in practice by the thermal expansion limitations imposed by tunnel structure. Since moisture condensation in supersonic flow is dependent upon pressure level, the variation of bellmouth pressure with Mach number for this particular tunnel is shown in figure 4.

The maximum heater temperature rise indicated in figure 3 results in a reduction of 0.023 in the specific heat ratio γ in pure air. Further changes existed because of the varying chemical composition of the heated airflow. Estimates of the composition were made at various temperature levels by assuming complete combustion of the natural-gas fuel. The amount of fuel needed was calculated from the required temperature increment and a heating value of 20 000 Btu per pound (46.49×10^6 J/kg). At the flight match conditions, or the design temperature limit, the required gas flow rate increased from 2.5 to 7.0 pounds per second (1.134 to 3.175 kg/sec) as the Mach number was increased from 2.0 to 3.5. Based on a balance of the chemical equations involved and the quantity of fuel used, the amount of combustion products and their effect on γ were determined. No attempt was made to determine experimentally the exact constituents of the resulting mixture. The theoretical variation in specific-heat ratio (calculated at free-stream total temperature) is presented in figure 5. This γ variation was used in computing both local Mach number and total pressure from the survey wedge pressure data. Since the products of combustion were a small percentage (7.5 percent maximum) of the total airflow, the γ change was primarily dependent on the final temperature and was relatively insensitive to the induced temperature increment at the various Mach numbers. At Mach 2.5, a reduction in temperature increment of approximately 85° R (47 K) due to secondary compressor operation changed the value of γ at flight temperature by about 0.0005. This change was not sufficient to show as a discontinuity on the curve of γ as a function of temperature (fig. 5), since it had no significant effect on the calculation of either Mach number or tunnel total pressure loss.

Figures 6(a) and (b) show the 17 calibration wedges spaced uniformly in a 4-foot-square pattern. Details of the construction and instrumentation of individual wedges are shown in figure 6(c). Total temperature was measured directly with an aspirating-type high-recovery thermocouple attached to each wedge. Local Mach number was obtained from the ratio of the wedge pitot pressure $\overline{P}_2$ (averaged from both sides of the 20° wedge) to the free-stream pitot pressure P_1 and from an iterative procedure involving the equations for the total pressure loss across a normal shock and the flow conditions across a two-dimensional oblique shock wave. A wedge angle of 20.5° was used in the calculations to account for the experimentally measured boundary-layer thickness on the wedge

surface. The local free-stream total pressure was determined from the local free-stream Mach number, the measured value of P_1, and the relation across a normal shock. Effects of γ change were included in the calculations; however, reevaporation of any water vapor behind shock waves was assumed to have no effect on the calculations. The average flow conditions at each station were obtained by a simple arithmetic average of the local values obtained from each individual wedge.

RESULTS AND DISCUSSION

The effect of heater operation on test-section Mach number is shown in figure 7. The flexible nozzle wall position was varied to provide a nominal Mach number range from 2.0 to 3.5 in increments of 0.1. At each nozzle position, total temperature was varied until it either exceeded the appropriate flight stagnation temperature or encountered the heater maximum temperature limit. In all cases, the average Mach number dropped initially as temperature increased; but at the higher temperatures, it reversed the trend and began to increase toward its original value. Presumably, this dip was the result of two conflicting tendencies: increased combustion increased the amount of water vapor present in the airflow, but at higher temperatures, the higher static temperatures limited the quantity of water vapor which was permitted to condense.

Wall static pressure distributions obtained through the nozzle and test section indicated that condensation generally began about 12 feet (3.66 m) downstream of the tunnel throat and, generally, was completed before entering the test section. Also, heater operation varied the details of very weak test-section wall static pressure gradients resulting from imperfect cancellation of expansion and compression waves in the nozzle; however, the maximum deviation was no greater than that observed during normal tunnel operation without the heater. The uniformity of the test-section flow is also well illustrated in figure 7 in that the downstream average Mach number was either indentical to the upstream value or was increased a small amount. This shift was most obvious, of course, at the highest Mach numbers where it would be more difficult to maintain uniform flow over this length of test section. In these cases, it is also thought that the $0^{\circ}22'$ divergence of each test-section side wall is larger than required to compensate for the boundary-layer growth since the downstream Mach number was greater than the upstream value.

The corresponding effects of heater operation on test-section total pressure are presented in figure 8. Here the ratio of test-section total pressure to bellmouth total pressure is shown for the identical operating conditions of figure 7. As expected, the largest total pressure loss occurred for those high Mach number and high temperature conditions causing the largest decrease in test-section Mach number. The only indication that some condensation effects occurred in the test section between the upstream and downstream positions can be seen at the higher temperatures. In these cases, the down-

stream total pressure loss was greater than that at the upstream survey station.

Theoretical calculations of the effect of water-vapor condensation on the pressure recovery of the tunnel were made for several temperatures at Mach 2.0, 2.5 (with secondary drive operating), and 2.9. For these computations it was assumed that the combustion efficiency was 100 percent and that all of the water vapor due to combustion condensed in a shock at the test-section Mach number. Starting with the undisturbed Mach number, free-stream temperature, and temperature increment due to the water-vapor condensation, the pressure decrement due to condensation effects was calculated by using the Rayleigh line. To account for the additional total pressure loss occurring during normal expansion of the flow through the nozzle, the computed ratios of free-stream total pressure to bellmouth total pressure were multiplied by the corresponding ratios which were measured without heater operation

$$\left(\frac{P_0}{P_B}\right)_{computed} \times \left(\frac{P_0}{P_B}\right)_{cold}$$

to find the overall ratio of the test-section total pressure to bellmouth total pressure. The results obtained by this method (fig. 8) are in good agreement with the measured values at temperatures below flight simulation. As indicated by the deviation from experimental results, the assumption of complete condensation at free-stream Mach number does not apply at the higher temperatures.

CONCLUDING REMARKS

Conditions causing moisture condensation in supersonic tunnel flow are normally shunned because large flow nonuniformities may result in the test section. However, it is apparent that with large wind tunnels, such as the 10- by 10-foot supersonic wind tunnel, vitiated air for temperature control can be used within limits without causing serious compromises in flow quality. In this particular tunnel design, the nozzle was of sufficient length that the condensation phenomenon was essentially complete upstream of the test section. Although the test-section Mach number and total pressure were decreased by this effect, the changes in flow conditions were repeatable and could be calibrated accurately. The products of combustion would never exceed 7.5 percent of the total airflow; therefore, no attempt was made to determine experimentally the exact constituents of the flow at the various heated conditions.

Lewis Research Center,
National Aeronautics and Space Administration,
Cleveland, Ohio, April 29, 1968,
126-15-02-11-22.

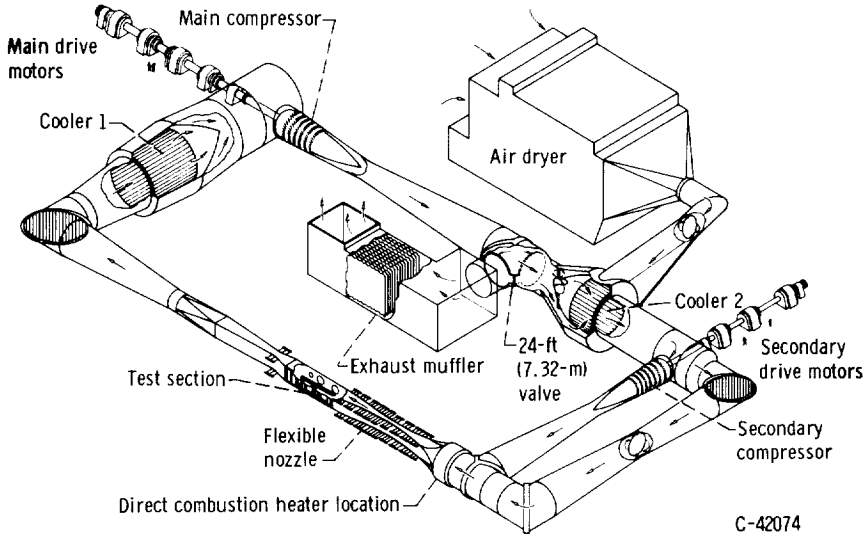

(a) Schematic diagram.

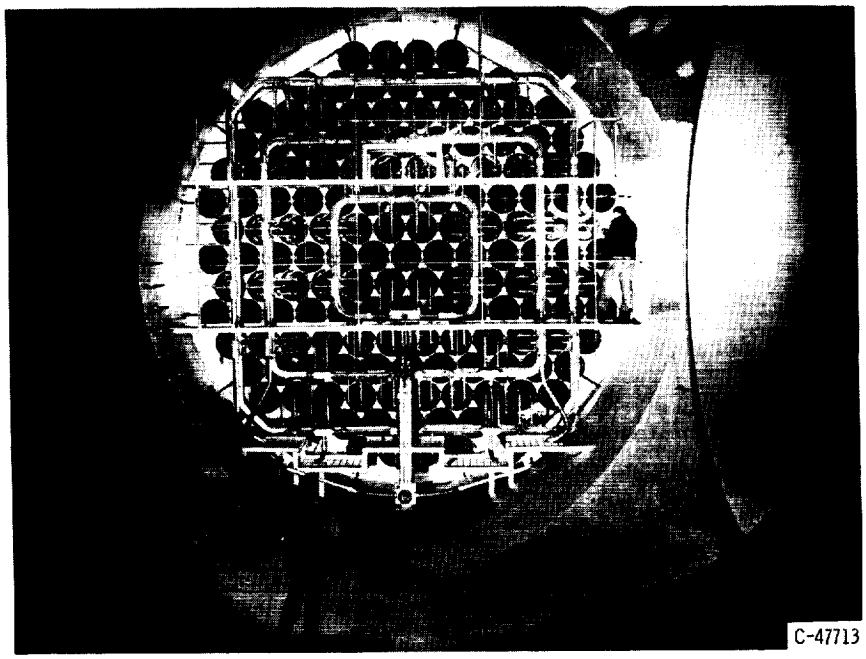

(b) Direct combustion heater.

Figure 1. - Lewis 10- by 10-foot supersonic wind tunnel.

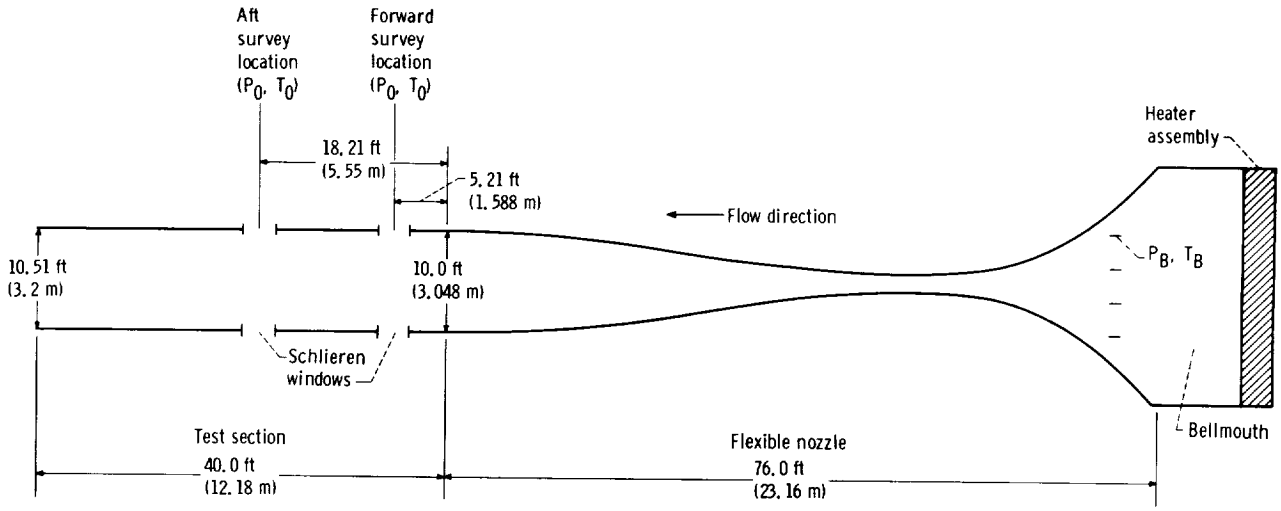

Figure 2. - Schematic diagram of 10- by 10-foot supersonic wind tunnel bellmouth, nozzle, and test section.

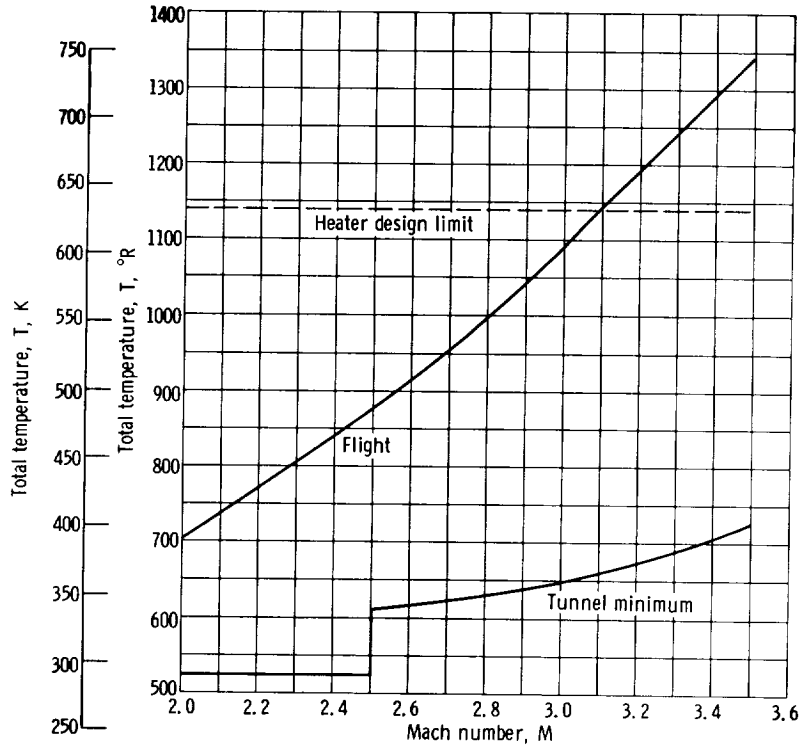

Figure 3. - Variation of required temperature rise of heater with Mach number of 10- by 10-foot supersonic wind tunnel.

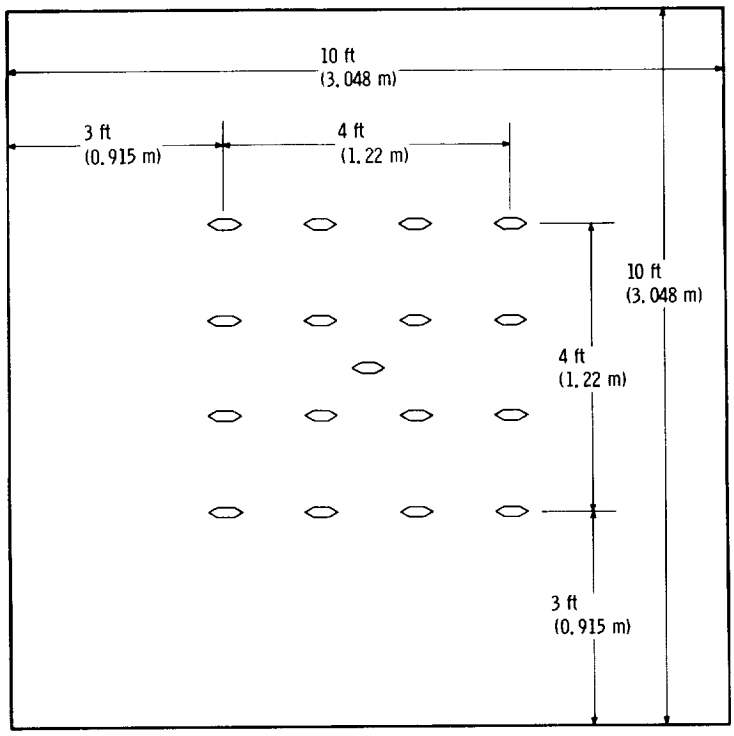

(b) Wedge arrangement in test section.

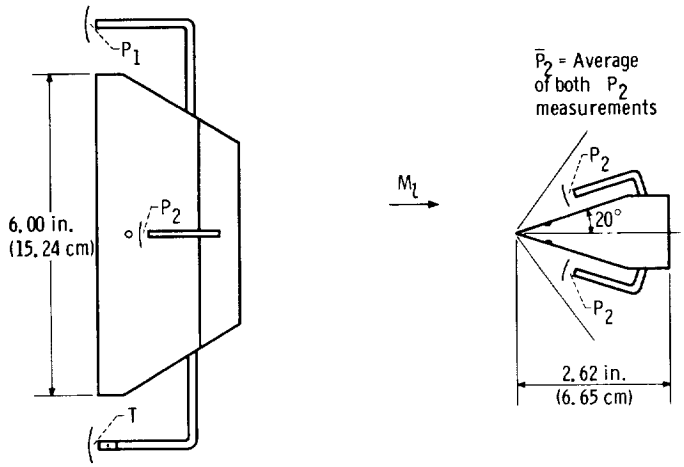

Top view

Side view

(c) Details of wedge design and instrumentation.

Figure 6. - Concluded.

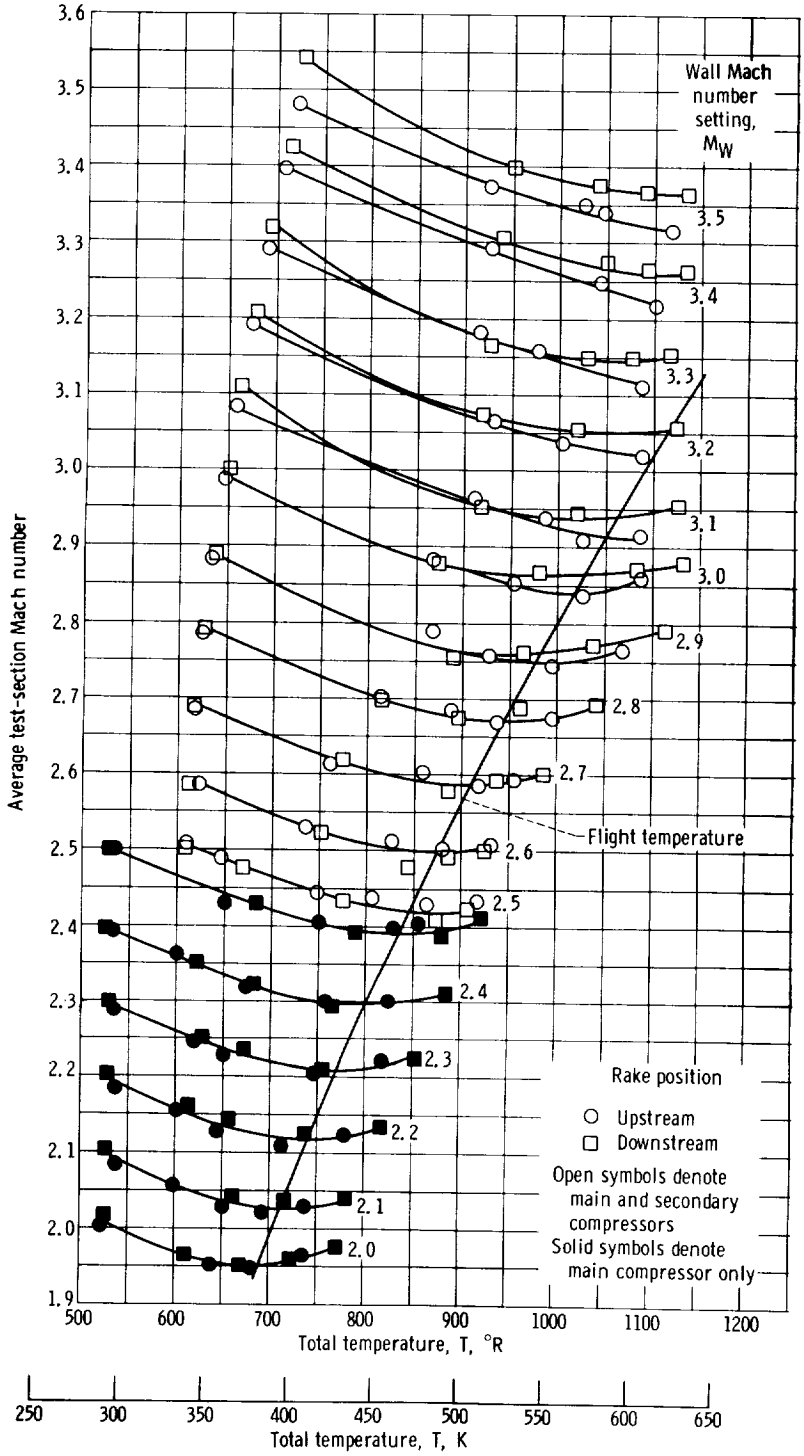

Figure 7. - Variation of 10- by 10-foot supersonic wind tunnel test section Mach number with total temperature.

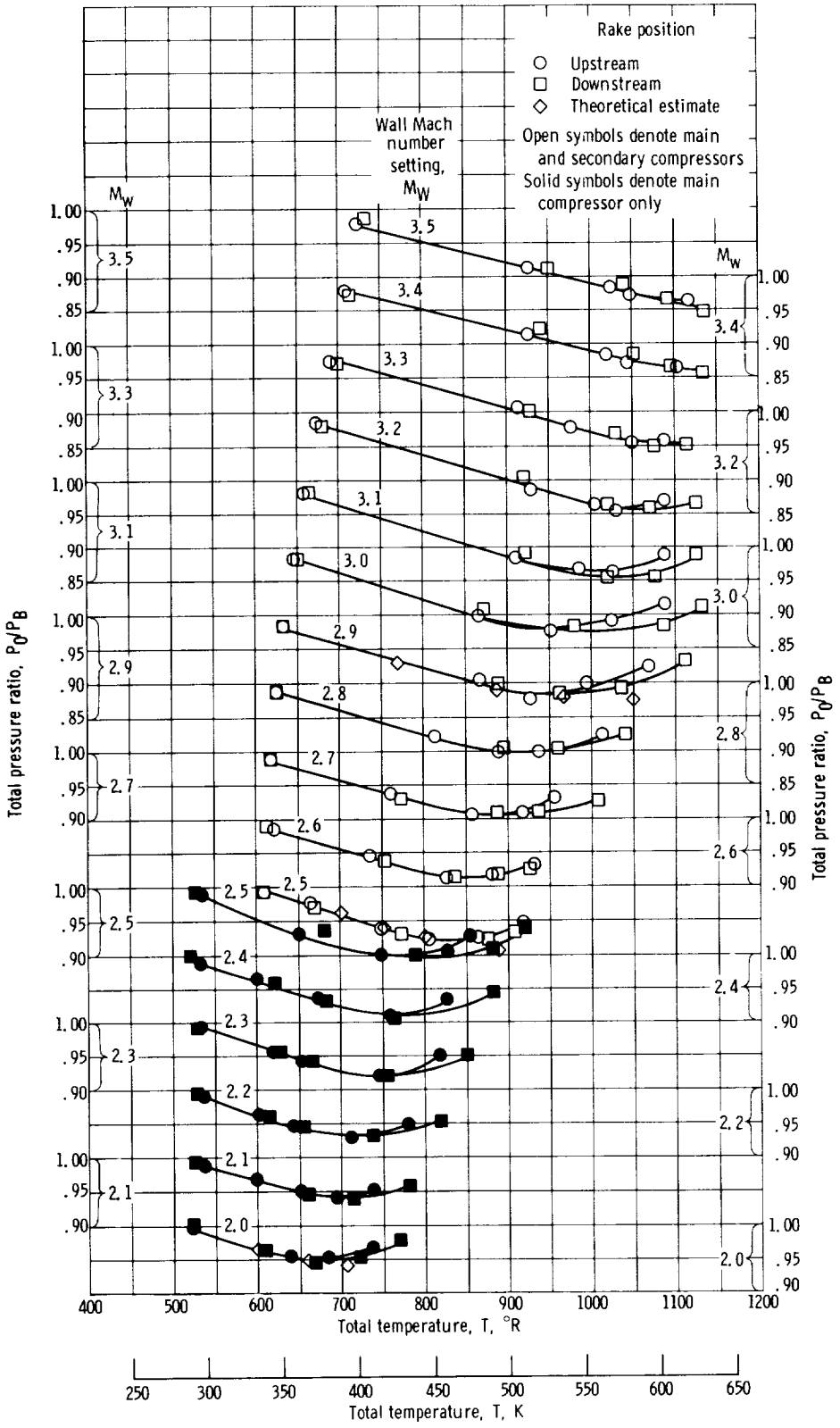

Figure 8. - Variation of 10- by 10-foot supersonic wind tunnel test section total pressure with total temperature.

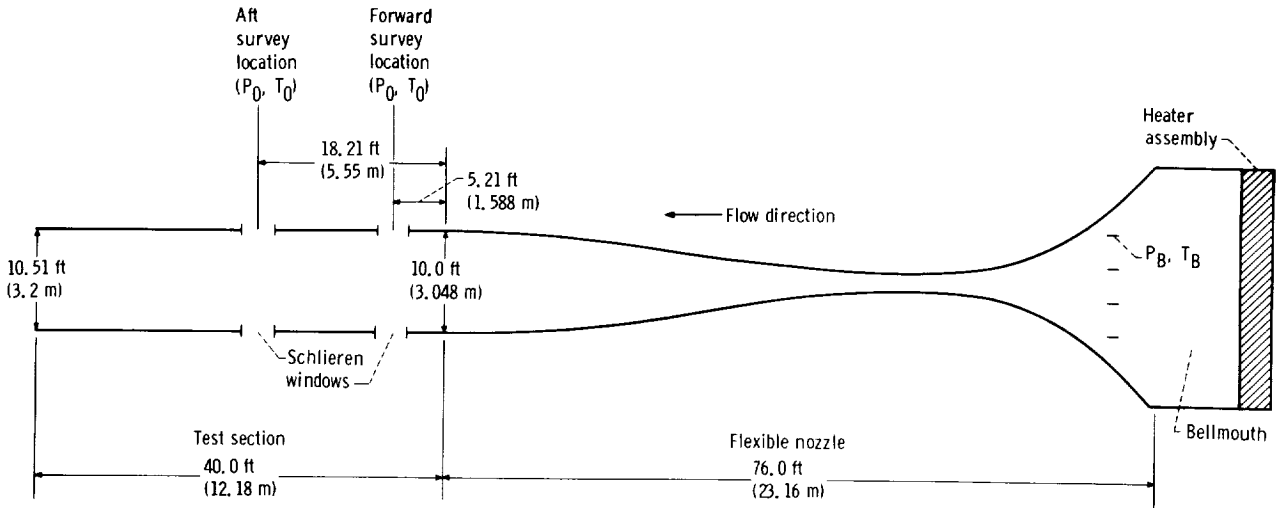

Figure 2. - Schematic diagram of 10- by 10-foot supersonic wind tunnel bellmouth, nozzle, and test section.

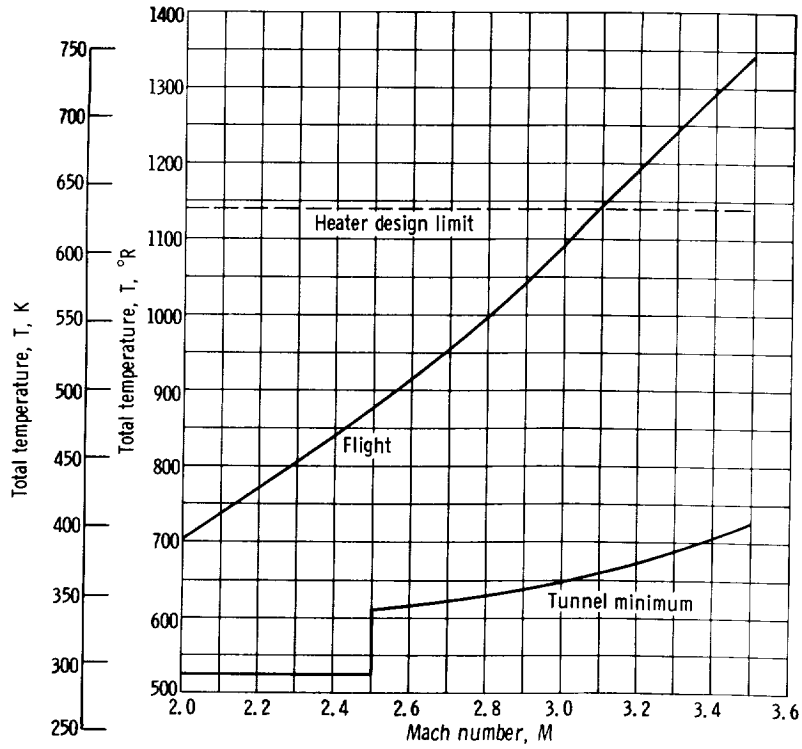

Figure 3. - Variation of required temperature rise of heater with Mach number of 10- by 10-foot supersonic wind tunnel.

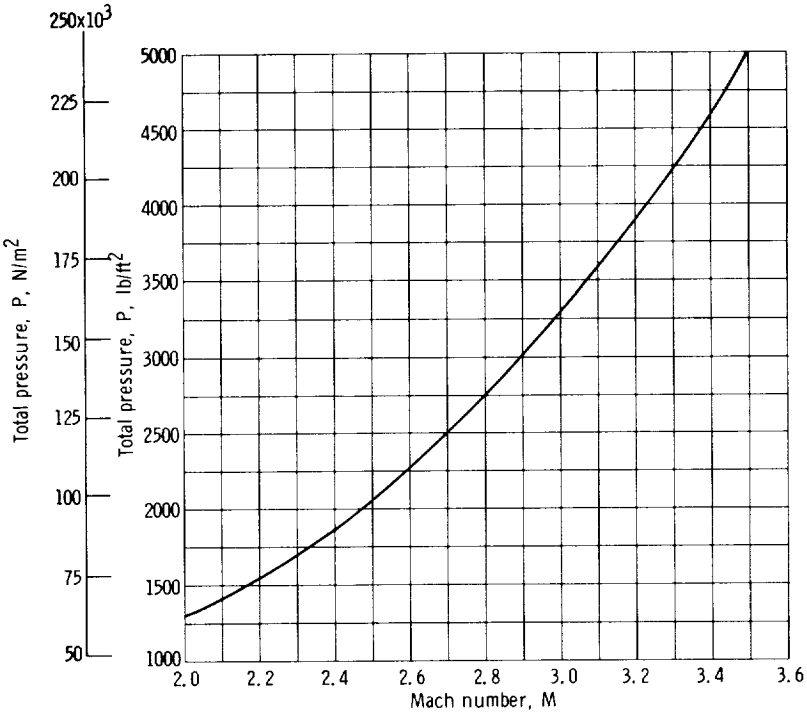

Figure 4. - Variation of bellmouth total pressure with Mach number for open-cycle operation of 10- by 10-foot supersonic wind tunnel.

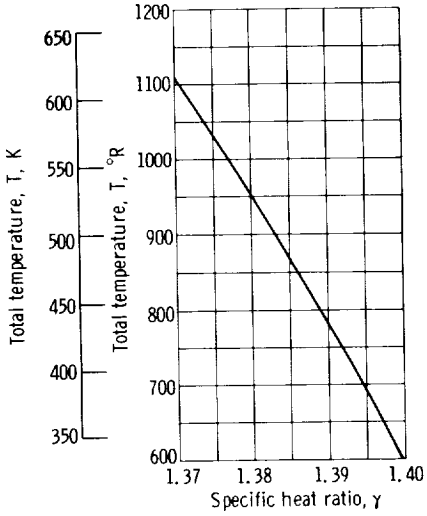

Figure 5. - Variation of specific heat ratio with temperature for 10- by 10-foot supersonic wind tunnel with heaters operating.

(a) Tunnel installation.

Figure 6. - Survey rake.

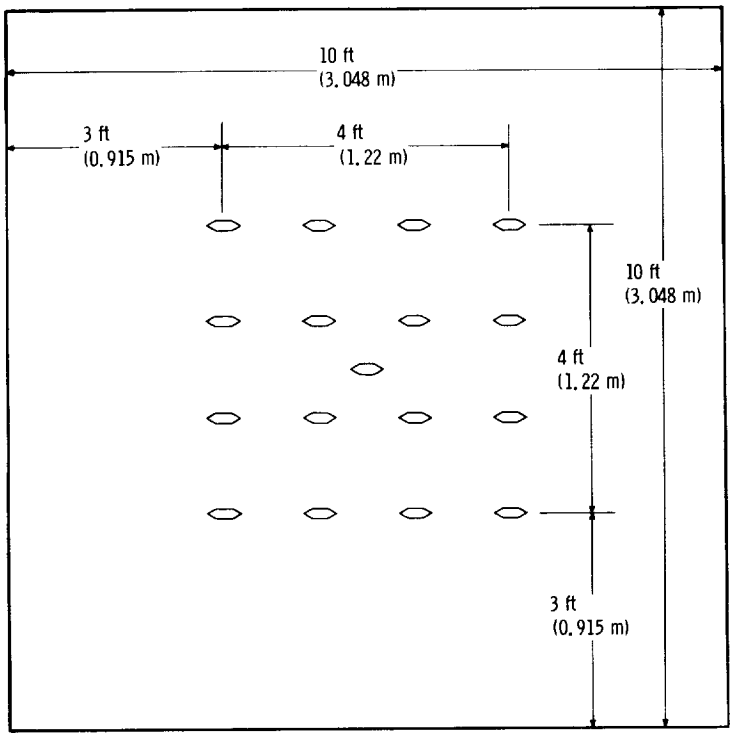

(b) Wedge arrangement in test section.

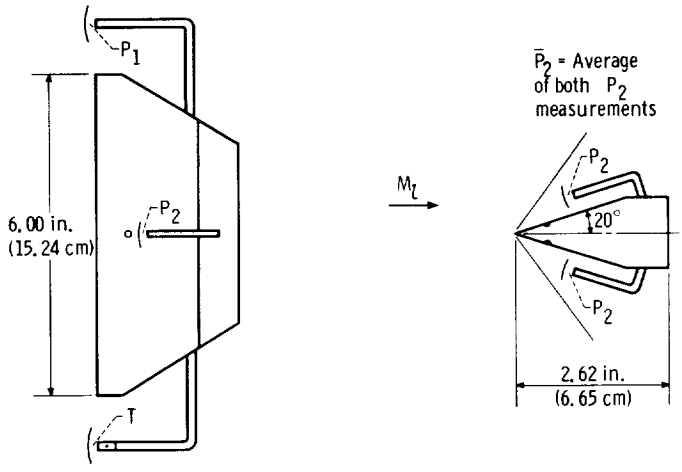

(c) Details of wedge design and instrumentation.

Figure 6. - Concluded.

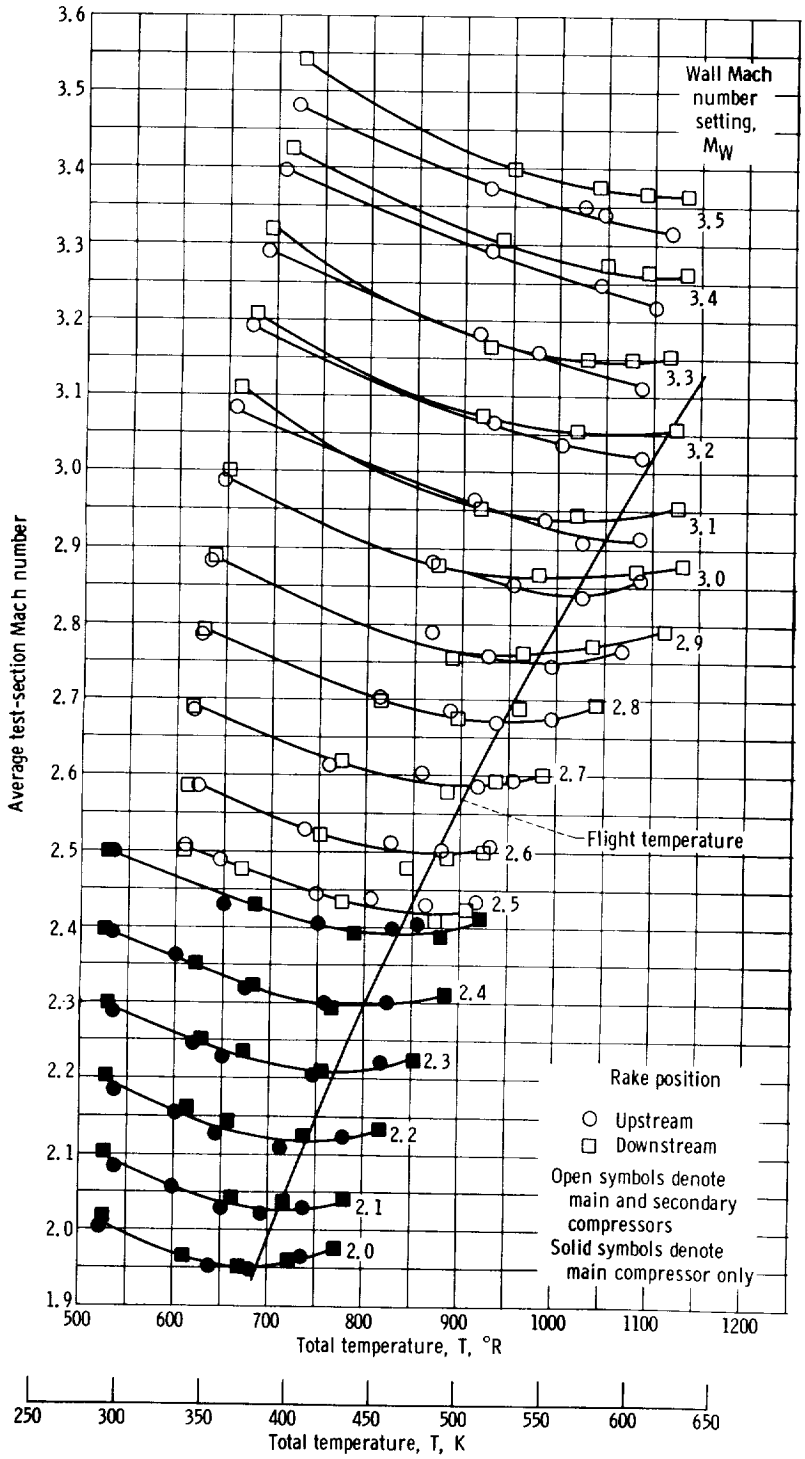

Figure 7. - Variation of 10- by 10-foot supersonic wind tunnel test section Mach number with total temperature.

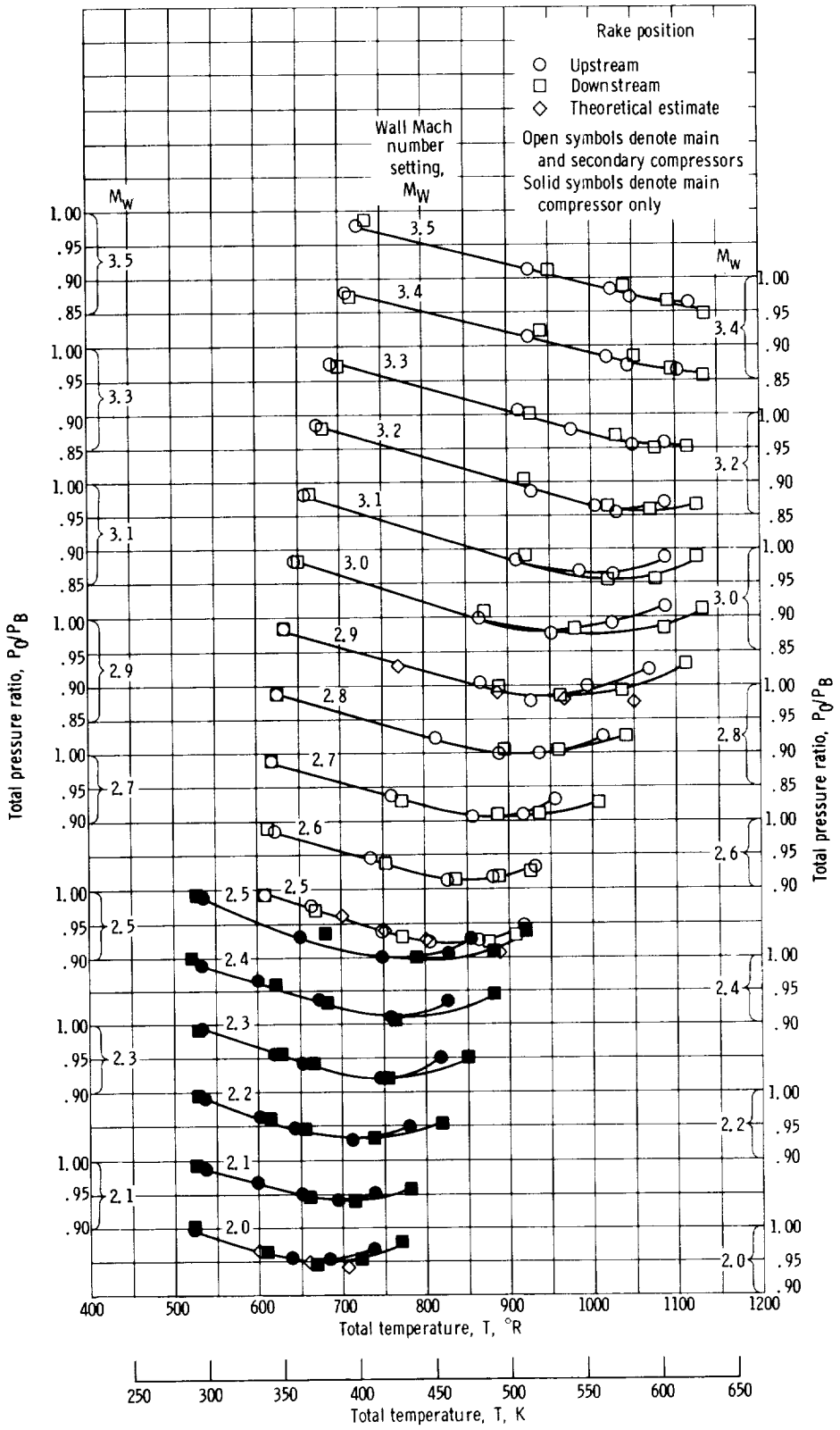

Figure 8. - Variation of 10- by 10-foot supersonic wind tunnel test section total pressure with total temperature.